Interfacial enhancement of ferroelectricity in CaTiO₃/BaTiO₃ superlattices

Xifan Wu,[1,*] Karin M. Rabe,[2] and David Vanderbilt[2]

[1]*Department of Physics, Temple Materials Institute, and Institute for Computational Molecular Science,*
Temple University, Philadelphia, Pennsylvania 19122, USA
[2]*Department of Physics and Astronomy, Rutgers University, Piscataway, New Jersey 08854-8019, USA*

We carry out first-principles calculations for $CaTiO_3$/$BaTiO_3$ superlattices with epitaxial strain corresponding to growth on a $SrTiO_3$ substrate, and consider octahedral rotations as well as ferroelectric distortions. The calculations are done as a function of electric displacement field, and both a macroscopic and a local electrostatic analysis are carried out. We find that strong octahedral rotations occur for TiO_6 octahedra sandwiched between CaO layers on both sides, but are strongly suppressed if either neighboring layer is a BaO layer. Due to the resulting enhancement of the ferroelectric instability in these octahedra, we find that overall the ferroelectric instability of the superlattice is enhanced by the interface. Thus, short-period superlattices in this system have a larger ferroelectric polarization than longer-period ones of the same average composition, contrary to the expected trend.

PACS number(s): 77.22.Ej, 77.80.−e, 77.84.Lf

ABO₃ perovskite oxide superlattices are currently the subject of intense scientific interest.[1–4] Through variation of the choice of constituent materials and their order of deposition, as well as the epitaxial strain state via selection of the substrate, a wide variety of functional properties can be achieved. While the properties can be understood partly as the result of the behaviors of the constituent materials under the electrical and mechanical boundary conditions characteristic of the superlattice,[2] in many cases the atomic and electronic features of the interfaces have been shown to play a critical role.[5] As a result, materials design via interface engineering is becoming an essential strategy in guiding experimental exploration of this enormous class of materials, and there is clearly a pressing need for improved atomic-scale understanding of the role played by the interfaces in determining the functional properties of perovskite superlattices.

First-principles methods have been extremely useful in providing both qualitative and quantitative characterization of interface effects in superlattices.[5,6] In most perovskite superlattices combining ferroelectric (FE) and paraelectric (PE) layers,[2,3,5,7–9] the FE instability and spontaneous polarization are found to be suppressed with increasing interface density for a given overall composition. In an analysis based on layer polarizations defined in terms of localized Wannier orbitals[6] and using electric displacement D as the fundamental field variable, the properties of interfaces were found to be determined mainly by the adjacent atomic layers.[5,10] In this local analysis, the suppression of ferroelectricity by interfaces was associated with the formation of an interface dipole pointing antiparallel to the local polarization.

An additional feature of many perovskite oxides is a tendency for rotations and tilts to occur in the corner-sharing network of oxygen octahedra. For example, the crystal structure of bulk CaTiO₃ (CTO) is generated by large oxygen octahedral rotations; its nonpolar character is thus understood as the result of the competition between FE and antiferrodistortive (AFD) orders, which suppresses the FE instability in the AFD state.[11] In contrast, BaTiO₃ (BTO) is highly resistant to oxygen octahedral rotations and

exhibits a robust FE state at room temperature.[12] Previous first-principles studies of the CTO/BTO superlattice system have neglected the oxygen octahedral rotations,[5,7,13] yielding an artificially strengthened ferroelectricity and an enhanced ground-state polarization[5,7] which increases as the interface density decreases. In contrast, a slight increase in polarization from the 2 : 2 to the 1 : 1 superlattice is observed in a recent experiment.[14]

In this paper we show that an increased density of interfaces can in fact enhance the polarization of a superlattice, illuminating the experimental observation of Ref. 14. The key to this unusual behavior is the role played by octahedral rotations, in addition to FE distortions, in determining the energetics and polarization of the interfaces.[4] Working with superlattices comprised of CTO and BTO layers as our model system, we use first-principles calculations to demonstrate this effect and to clarify the reasons for its occurrence. We find that the octahedral rotations are large for TiO_6 octahedra sandwiched between CaO layers, but are strongly suppressed if either neighboring layer is a BaO layer. The latter case results in a local enhancement of the FE instability and of the resulting polarization. As a result, short-period superlattices, in which the density of interfaces is higher, have a larger spontaneous polarization than longer-period ones of the same average composition.

The details of the calculations are as follows. We carry out strained-bulk calculations on all distinct period-4-compatible superlattices built from CaTiO₃ (C) and BaTiO₃ (B) cell layers, namely, BTO, 3B1C, 2B2C, 1B1C, 1B3C, and CTO, stacked in the [001] direction. The in-plane lattice constant is fixed at $a_0 = 7.275$ bohr, our computed equilibrium lattice constant for bulk cubic SrTiO₃, corresponding to epitaxial growth on SrTiO₃. We use a 40-atom tetragonal supercell with lattice vectors of length $\sqrt{2}a_0$ in the [110] and [1$\bar{1}$0] directions and $c \approx 4a_0$ along the [001] direction. This allows us to consider both the FE distortion along [001] and an antiferrodistortive pattern of octahedral rotations about the [001] axis, resulting in $P4bm$ space-group symmetry. We neglect the tilting of oxygen octahedra (rotations about an in-plane axis); we believe this

TABLE I. Computed tetragonal distortion ($c/4a_0$) and spontaneous polarization, in C/m^2, of the CTO/BTO supercells, with (P_s) and without ($P_{s,0}$) octahedral rotations.

	BTO	3B1C	1B1C	2B2C	1B3C	CTO
P_s	0.388	0.333	0.184	0.161	0.0	0.0
$c/4a$	1.0595	1.0359	1.0114	1.0110	0.9939	0.9798
$P_{s,0}$	0.388	0.346	0.266	0.374	0.447	0.590

is justified because oxygen tilting requires a coherent pattern of tilts that would propagate into the BTO unit cells, where octahedral rotations are unfavorable.

The structural relaxations and electron minimizations were done at fixed electric displacement fields within the framework of density-functional theory in the local-density approximation[15] using the LAUTREC code package,[10] which implements plane-wave calculations in the projector augmented-wave framework.[16] We used a plane-wave cutoff energy of 80 Ry and a $4 \times 4 \times 1$ Monkhorst-Pack k mesh.

In Table I we present the spontaneous polarization P_s and c/a ratio for each of the six superlattices considered. As expected, P_s increases with increasing BTO fraction. Comparing the two superlattices 2B2C and 1B1C, which have the same overall composition, we find that the latter, with higher interface density, has a larger P_s, contrary to the expectations based on FE-PE superlattices previously considered in the literature,[2,5,7] but consistent with the experimental result reported in Ref. 14. This enhancement in 1B1C, however, is not due to improper ferroelectricity as was the case for PbTiO$_3$/SrTiO$_3$ described in Ref. 4. In both 1B1C and 2B2C, the rotations suppress, rather than enhance, the polarization, as can be seen by comparing the polarization in the presence of rotations with the polarization computed for rotations constrained to zero, given in the last row of Table I. Although the polarization in the absence of rotations is much greater for 2B2C, reflecting the expected trend in which a higher interface density suppresses the polarization, the magnitude of the suppression by rotations is much greater for 2B2C than for 1B1C, due to the large rotation angle in the CC layer. The net result is to reverse the trend, with the polarization in 1B1C with rotations being slightly larger than for 2B2C. Application of a large electric field, as in Ref. 13, is expected to favor states with higher polarization and smaller octahedral distortion, reflecting the competition between these two distortions; this could be investigated by application of the present approach but will not be further discussed here.

To develop an atomic-scale understanding of the enhancement of the polarization in 1B1C, we carry out a layer-by-layer analysis of structural and dielectric properties of the superlattices.[5,6] In previous work,[5] we showed that the properties of each atomic layer depend only on the chemical identity of neighboring layers and on global parameters such as the in-plane lattice constant and the displacement field D (along z). We expect this "locality principle" to continue to apply when the AFD rotations are included in the analysis. In Fig. 1 (relative to the corresponding average of TiO$_2$ layers in bulk CTO and BTO), we plot the layer polarizations of TiO$_2$ layers as a function of D for all the CTO/BTO supercells considered. For each D, we fully relax the structure, optimizing
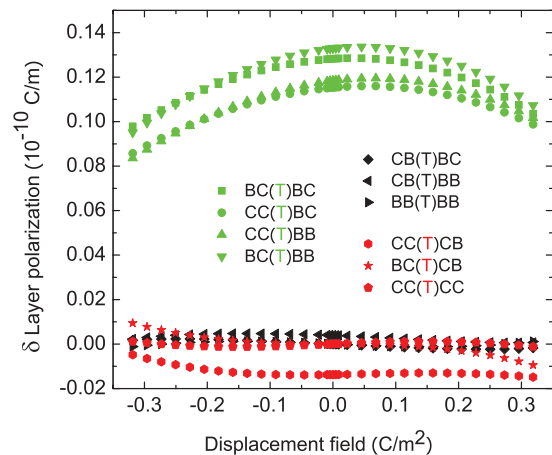

FIG. 1. (Color online) Dependence of TiO$_2$ layer polarizations (relative to the average of TiO$_2$ planes in bulk BaTiO$_3$ and CaTiO$_3$) on chemical environment in CTO/BTO supercells.

with respect to rotations of the octahedra in each layer. It can be seen that the layer polarizations are mainly determined by the chemical identity of the first-neighbor layers, just as was the case when octahedral rotations were constrained to zero.[5]

We next consider the octahedral rotations and show that these, too, are functions of the local chemical environment in a similar way as for the layer polarizations. In all of the CTO/BTO superlattices studied here, we found that structures having rotations that change phase from layer to layer have lower energy than those with in-phase rotations. Henceforth we characterize the structures by the absolute value θ_j of the rotation angle for TiO$_2$ layer j, with the understanding that the signs always alternate from layer to layer.

The calculated dependence of the rotation angles on D is presented in Fig. 2. The results are grouped into three categories depending on whether the two first-neighbor AO layers are both CaO, one CaO and one BaO, or two BaO layers. It is clear that the octahedral rotations depend strongly on the identity of the first-neighbor layers, while the influence of the second-neighbor layers is much weaker. A closer inspection shows that a large octahedral rotation of $\sim$12°–13° is observed whenever the TiO$_6$ layer is sandwiched by two CaO layers, while only a tiny rotation is found for the TiO$_6$ octahedra sandwiched between BaO layers. This is consistent with the properties of the parent materials, since rotations are strongly favored in bulk CTO while being suppressed in bulk BTO. We find that the D-field dependence of the octahedral rotations is generally weak in both cases.

What is more intriguing, however, is the behavior of the interfacial layers of TiO$_6$ octahedra. These experience a strongly broken mirror symmetry due to the presence of BaO on one side and CaO on the other. The rotation angles are intermediate in size, $\sim$4°–6°, and are much more strongly dependent[17] on D. [A similar effect due to second-neighbor asymmetry, barely visible for some of the curves in Figs. 2(a) and 2(c), has a very much weaker amplitude.] It is this reduction in the angle that allows a larger polarization to develop in this layer, enhancing the overall polarization of the system.
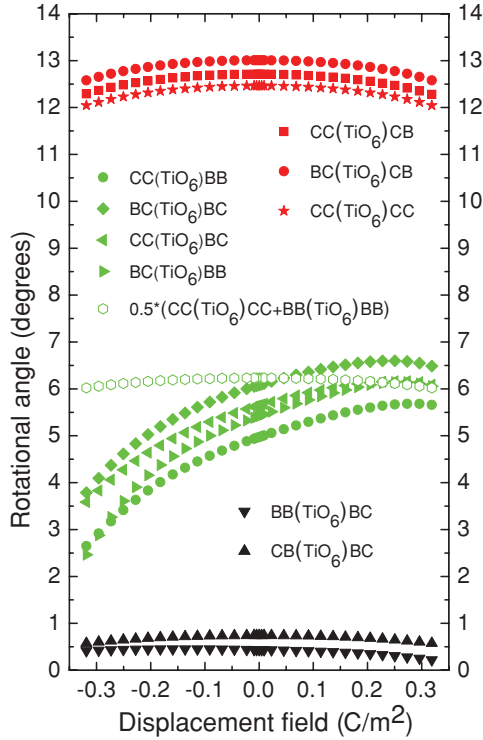
FIG. 2. (Color online) TiO$_6$ rotation angles as a function of D field for TiO$_6$ octahedra sandwiched between (a) two CaO layers, (b) one BaO and one CaO layer, and (c) two BaO layers.

This behavior can also be analyzed by examining the tendency of a system toward ferroelectric behavior as measured by the inverse permittivity $\epsilon^{-1} = \partial E/\partial D$ evaluated at $D = 0$,[10] where E is the electric field. This is positive for a PE system, goes smoothly to zero as the system approaches a FE instability, and is negative for a FE material. Thus, $\epsilon^{-1}(D = 0)$ provides information that is complementary to the spontaneous polarization, providing a measure of proximity to a FE instability in PE systems and of the strength of the instability in FE systems that is independent of higher-order terms.

With this motivation, we present in the third column of Table II the inverse permittivities ϵ^{-1} at $D = 0$ for our bulk and superlattice structures for the case that rotations are allowed. As expected, the (strained) bulk BTO shows the most FE behavior (strongly negative ϵ^{-1}), while the (strained) bulk CTO remains PE ($\epsilon^{-1} > 0$). The dielectric responses of the mixed superlattices are thus intermediate between those of bulk BTO or CTO, as expected. Consistent with the interface density dependence of the polarization, we find that the FE instability of the 1B1C superlattice is slightly greater than that of the 2B2C superlattice, and both of these are greater than the average of BTO and CTO, which corresponds to nBnC in the limit $n \to \infty$ and interface density equal to zero.

The emergence of this interface enhancement effect is related to the coexistence of FE and AFD order in the system. To demonstrate this, the last column of Table II presents the inverse dielectric permittivities with octahedral rotations constrained to zero. Here, we find that bulk CTO has nearly the same degree of FE instability as bulk BTO, while the

TABLE II. Reduced inverse dielectric permittivities $\epsilon_r^{-1} = \epsilon_0/\epsilon$ computed at $D = 0$ for the bulk and supercell structures studied.

Superlattice	CaTiO$_3$ fraction	Rotations allowed	Rotations forbidden
BTO	0	−0.0191	−0.0191
3B1C	0.25	−0.0118	−0.0108
1B1C	0.50	−0.0030	−0.0039
2B2C	0.50	−0.0028	−0.0074
1B3C	0.75	0.0063	−0.0070
CTO	1	0.0157	−0.0151

presence of interfaces reduces the FE instability substantially for the 3B1C, 2B2C, and 1B3C superlattices, and even more for the 1B1C superlattice, with a twofold increase in interface density. Comparing with the values when rotations are allowed, it is clear that the suppression of the octahedral rotation greatly increases the FE tendency in the supercells involving 50% or more CTO.

From these comparisons, it follows that the competition between AFD and FE orders is essential for the interface enhancement effect in this system. In fact, there is a local relationship between the octahedral rotations in a layer and their contribution to the FE instability. For the purposes of carrying out a local decomposition, we focus on the inverse of the capacitance per basal area, $C^{-1} = \partial V/\partial D$, at $D = 0$. Here $V = LE$ is the potential drop across the supercell, with L being the supercell height in the stacking direction and E the average electric field. Apart from a small correction proportional to $\partial L/\partial D$, which we have verified has little effect on the analysis, this is equal to $L\epsilon^{-1}$, and thus can be used as a measure of ferroelectric instability similar to ϵ^{-1}.[10] We decompose C^{-1} locally as follows. First, for each AO or TiO$_2$ layer in the superlattice, we define an inverse layer capacitance

$$c_j^{-1} = \frac{1}{\epsilon_0}\left(h_j + D\frac{\partial h_j}{\partial D} - \frac{\partial p_j}{\partial D} \right), \quad (1)$$

where h_j and p_j are the layer height[18] and layer polarization[6] associated with each layer j. We then assign an inverse cell capacitance to the cell centered on TiO$_2$ layer i as

$$C_i^{-1} = c_{\text{TiO}_2,i}^{-1} + \tfrac{1}{2}c_{\text{AO},i-1}^{-1} + \tfrac{1}{2}c_{\text{AO},i+1}^{-1}. \quad (2)$$

Taking the 2B2C supercell as an example, we report the resulting inverse cell capacitances at $D = 0$ in Table III. The last column of the table is $C_{\text{tot}}^{-1} = \sum_{i=1}^{4} C_i^{-1}$. For comparison, the results are given both for the case that rotations are allowed and when they are forbidden. As expected, the absence of the oxygen rotations results in a much stronger FE instability, as shown by the fact that C_{tot}^{-1} is much more negative than when rotations are allowed. The individual inverse cell capacitances show changes in Table III that are not always easy to interpret, because the inverse capacitance of a given TiO$_2$-centered unit cell does still depend fairly strongly on the identity of neighboring cells. For example, $C_{\text{B(T)B}}^{-1}$ is not independent of environment, despite the fact that the rotations in that TiO$_2$ layer are quite small. However, there is one huge change that stands out in Table III, namely, that $C_{\text{C(T)C}}^{-1}$, the inverse capacitance of the cell containing the octahedra sandwiched

TABLE III. Inverse cell capacitance (J m^2/C^2) at $D = 0$ for each TiO$_2$-centered unit cell in the 2B2C supercell, for the case that rotations are allowed ($P4bm$ symmetry) or forbidden ($P4mm$ symmetry).

	$C^{-1}_{B(T)B}$	$C^{-1}_{B(T)C}$	$C^{-1}_{C(T)C}$	$C^{-1}_{C(T)B}$	C^{-1}_{tot}
$P4bm$	−0.416	−0.361	0.663	−0.361	−0.475
$P4mm$	−0.007	−0.152	−0.985	−0.152	−1.296

between CaO layers, changes drastically when rotations are allowed. Here, the oxygen rotation angle is ∼13°, similar to what it is in bulk CTO, and this induces an enormous suppression of the FE instability in that layer, switching the local tendency from a ferroelectric to a strongly PE one.

These observations help explain the result presented earlier in the paper: that short-period superlattices can be more FE than long-period ones. We can expect that there are two competing influences: (i) the effect that typically occurs in FE-PE perovskite oxide superlattices in which the presence of an interface interrupts the FE order and reduces the FE tendency; and (ii) an effect that is driven by oxygen octahedral rotations and arises because of the severe suppression of ferroelectricity that occurs only for TiO$_6$ octahedra sandwiched between Ca layers on both sides. The density of such layers in an nBnC superlattice is $(n − 1)/2n$, or $1/2n$ less than in the average of bulk BTO and CTO. This $1/2n$ reduction of a suppressing influence amounts to an enhancement of the FE tendency in short-period superlattices. Effects (i) and (ii) are of opposite signs but evidently have similar magnitudes, with (ii) dominating. This accounts for the increase in polarization for the increased interface density of the 1 : 1 superlattice relative to the 2 : 2 superlattice, as observed in a recent experimental investigation.[14]

In conclusion, we have shown that oxygen octahedral rotations must be included for any realistic modeling of CTO/BTO superlattices. Using first-principles calculations, we find that the octahedral rotations in a given layer depend strongly on the local environment, i.e., on the identity of the neighboring layers. In particular, the rotational angle in a TiO$_2$ layer sandwiched between two CaO layers is found to be very large, while the one between two BaO layers rotates hardly at all, similar to the tendencies of the corresponding bulk CTO and BTO parent materials. The competition between rotations and ferroelectricity then plays out locally, and results in a behavior in which the ferroelectricity is found to increase systematically with decreasing n in nBnC superlattices, in contrast to what has been found when only the FE degrees of freedom are present. While the competition between antiferrodistortive oxygen octahedron rotations and ferroelectricity is the best studied, other competitive interactions between ferroelectricity, antiferrodistortive rotations, and other orderings such as antiferroelectricity and magnetic ordering have also been identified. Our results suggest that the investigation of superlattices with other competing interactions at the interface could reveal enhancements of a variety of functional properties. These results have critical implications for the design and application of short-period superlattice structures having enhanced or different properties.

*xifanwu@temple.edu

[1] N. Sai, B. Meyer, and D. Vanderbilt, Phys. Rev. Lett. **84**, 5636 (2000).

[2] J. B. Neaton and K. M. Rabe, Appl. Phys. Lett. **82**, 1586 (2003).

[3] H. N. Lee *et al.*, Nature (London) **433**, 395 (2005).

[4] E. Bousquet *et al.*, Nature (London) **452**, 732 (2008).

[5] X. Wu, M. Stengel, K. M. Rabe, and D. Vanderbilt, Phys. Rev. Lett. **101**, 087601 (2008).

[6] X. Wu, O. Diéguez, K. M. Rabe, and D. Vanderbilt, Phys. Rev. Lett. **97**, 107602 (2006).

[7] S. M. Nakhmanson, K. M. Rabe, and D. Vanderbilt, Phys. Rev. B **73**, 060101(R) (2006).

[8] K. Johnston, X. Huang, J. B. Neaton, and K. M. Rabe, Phys. Rev. B **71**, 100103(R) (2005).

[9] J. H. Lee, J. Yu, and U. V. Waghmare, J. Appl. Phys. **105**, 016104 (2009).

[10] M. Stengel, N. Spaldin, and D. Vanderbilt, Nature Phys. **5**, 304 (2009); M. Stengel, D. Vanderbilt, and N. Spaldin, *ibid.* **8**, 392 (2009); Phys. Rev. B **80**, 224110 (2009).

[11] D. Vanderbilt and W. Zhong, Ferroelectrics **206**, 181 (1997).

[12] W. Zhong, D. Vanderbilt, and K. M. Rabe, Phys. Rev. Lett. **73**, 1861 (1994).

[13] J. Y. Jo, R. J. Sichel, H. N. Lee, S. M. Nakhmanson, E. M. Dufresne, and P. G. Evans, Phys. Rev. Lett. **104**, 207601 (2010).

[14] S. Seo and H. N. Lee, Appl. Phys. Lett. **94**, 232904 (2009).

[15] J. P. Perdew and Y. Wang, Phys. Rev. B **45**, 13244 (1992).

[16] P. E. Blöchl, Phys. Rev. B **50**, 17953 (1994).

[17] The positive slope results from the fact that $D < 0$ pushes the interfacial TiO$_6$ octahedra into closer contact with the BaO layer, which tends to suppress rotation.

[18] The height h_j of layer j is defined as $(\bar{Z}_{j+1} − \bar{Z}_{j−1})/2$, where $\bar{Z}_j$ is the average [001] coordinate of all ions belonging to layer j.